ELSEVIER

Journal of Nuclear Materials 290–293 (2001) 588–592

journal of nuclear materials

www.elsevier.nl/locate/jnucmat

# Performance of high triangularity plasmas as the volume of the secondary divertor is varied in DIII-D

M.E. Fenstermacher [a,b,*], T.H. Osborne [b], T.W. Petrie [b], R.J. Groebner [b], C.J. Lasnier [a], R.J. La Haye [b], A.W. Leonard [b], G.D. Porter [a], J.G. Watkins [c], DIII-D Team

[a] *Lawrence Livermore National Laboratory, Livermore, CA 94551, USA*

[b] *General Atomics, P.O. Box 85608, San Diego, CA 92186-5608, USA* [1]

[c] *Sandia National Laboratories, P.O. Box 5800, Albuquerque, NM, USA*

**Abstract**

This paper examines the sensitivity of edge pedestal and divertor performance parameters to changes in the volume of a secondary divertor that tends to form inside the vacuum chamber in high triangularity plasma shapes. The sensitivity was examined by varying the vertical distance of the secondary *X*-point from the target plate, $Z_X^S$, while holding the primary *X*-point height fixed. The ion $\nabla B$ drift was in the direction of the primary divertor. Discharges with and without active primary divertor cryo-pumping were examined. The effective rate of rise of the core density at the L–H transition increased 80% as $Z_X^S$ was reduced. At high density achieved by gas injection, the core line-averaged density at the H–L back transition decreased by 30% as $Z_X^S$ was reduced. Both of these results indicate that performance may be affected when core plasma screening of neutrals in the secondary divertor is reduced as $Z_X^S$ decreases. The peak heat flux in the secondary divertor decreased as $Z_X^S$ was reduced due to increased flux expansion until a threshold was reached at $Z_X^S \sim 3$ cm where it remained constant. This indicated that the high recycling character of the plasma above the target in the secondary divertor was lost when the length of the outer divertor leg was reduced below a critical value. 

*Keywords:* Divertor; Plasma properties

## 1. Introduction

The design of any future tokamak begins with a decision on the shape of the core and divertor plasmas [1]. The desire is to achieve the performance advantages of high triangularity (high-$\delta$) operation [2] with the core plasma volume maximized and the divertor volume minimized. However, there is very limited data from systematic experiments to guide the decision on the optimum plasma shape [3].

This paper describes experiments that have increased our understanding of the complex coupling of core plasma performance to plasma cross-section and divertor plasma shape. Systematic shape variation experiments were done using Type I [4] ELMing H-mode plasmas in DIII-D (see Fig. 1). The response of core, pedestal, scrape-off-layer (SOL), and divertor plasma performance was examined versus triangularity, $\delta$ [5], up/down magnetic balance [6], and secondary divertor volume as described below.

This paper reports on a series of high-$\delta$ H-mode discharges in DIII-D in which the effect of variation in the secondary divertor volume on edge pedestal and divertor performance was examined (see inset in Fig. 2). At low $\delta$ in single-null (SN) divertor configurations, only the primary *X*-point is present inside the vacuum vessel. As $\delta$ is increased for fixed PF coil set the location of the secondary *X*-point, which maps at the midplane to a flux

* Corresponding author. Tel.: +1-858 455 4159; fax: +1-858 455 4156.

*E-mail address:* max.fenstermacher@gat.com (M.E. Fenstermacher).

[1] Correspondence address.

0022-3115/01/$ - see front matter 
PII: S0022-3115(00)00526-2

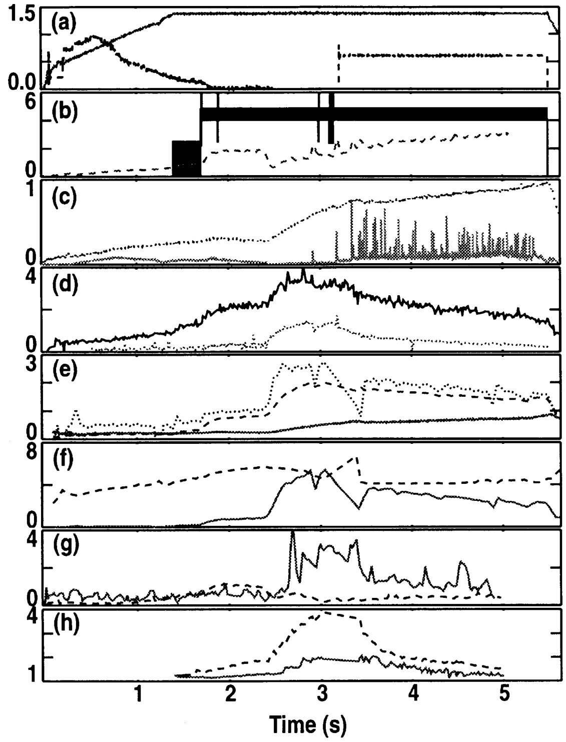


Fig. 1. Typical evolution of discharge parameters: (a) plasma current $I_p$ [MA] (solid) and gas injection [100 T$\ell$/s] (dashed); (b) injected beam power [MW] (solid) and radiated power [MW] (dashed); (c) $D_\alpha$ signal (solid), line-averaged density [$10^{20}$ m$^{-3}$] (dotted); (d) electron temperature [keV] – central (solid), pedestal (dotted); (e) fraction of Greenwald density (solid), $\beta_N$ (dashed), enhancement, $H_{89P}$, over ITER89P confinement [5] (dotted); (f) $\beta_N H_{89P}$ (solid) and 4 $\ell_i$ (dashed); (g) peak heat flux [MW/m$^2$] – upper divertor (solid) and lower divertor (dashed); (h) $Z_{eff}$ – central (solid) and edge (dashed).

surface radially outboard of the primary, tends to move from outside the vacuum vessel to inside and divertor physics (recycling, target heat flux, etc.) can become important in this secondary divertor. The studies were done by varying the height of the secondary (lower) $X$-point from the target plane, $Z_X^S$ in Fig. 2. Since the volume within the vacuum vessel that is made unavailable to the core plasma by the presence of a divertor scales with $Z_X^S$, the focus of the study was to determine the minimum $Z_X^S$ consistent with good core, pedestal and divertor performance.

The data showed that the presence of a second $X$-point in these unbalanced double-null (DN) shapes does not degrade the plasma performance if the secondary $X$-point is sufficiently far inside the vacuum vessel. These results, combined with those of Osborne et al. [5], and Petrie et al. [6] indicate that for high-$\delta$ operation an unbalanced DN shape has some advantages over a SN shape for future high power tokamak operation.

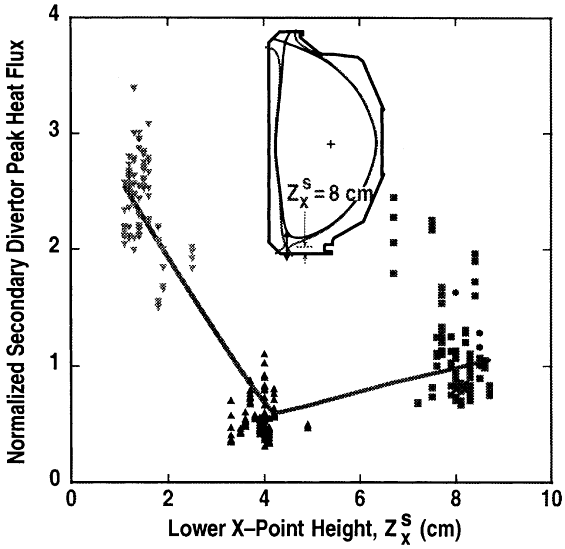


Fig. 2. Normalized peak heat flux in secondary divertor versus secondary $X$-point height, $Z_X^S$. Data are multiple samples from the ELMing H-mode period of three discharges (squares, upper triangles and lower triangles). Peak heat flux was normalized to expected value for $Z_X^S = 16$ cm and constant up/down magnetic balance. Peak heat flux decreases initially as $Z_X^S$ decreases due to flux expansion, then increases as high recycling character of secondary divertor is lost at low $X$-point height.

## 2. Description of experiments

The plasmas used in these experiments were operating in standard Type I ELMing H-mode [4] with neutral beam injection. No special profile control techniques were used and the radial profiles of the core plasma parameters (density, temperature, current, impurities) were typical of an ELMing H-mode well above the power threshold. Time histories of typical discharge parameters are shown in Fig. 1. Discharge parameters held constant throughout the scans of $Z_X^S$ were: plasma current, $I_p = 1.4$ MA, toroidal field, $B_T = 2.0$ T, major radius, $R_0 = 1.75$ m, minor radius, a $=$ 0.6 m, and injected neutral beam power, $P_{inj} = 4.6$ MW. Given the sensitivity of the divertor performance to variations in up/down magnetic balance shown in [6], an attempt was made to hold the magnetic balance constant as the secondary divertor volume varied. However, some up/down balance variation occurred and the results of Petrie et al. [6] have been used in the analysis below to try to distinguish the effect of divertor volume variation from the effect of up/down balance variation. Finally, the unpumped plasmas had an average triangularity, $\delta = 0.75$ and the pumped plasmas had $\delta = 0.6$. Elongation varied in the range of $\kappa = 1.88$–$2.15$ and this produced a variation in safety factor at the 95% flux surface, $q_{95} = 4.6$–$5.4$.

The goal of the discharges in this study was to examine the performance variations as a function of density within each shot and as a function of secondary divertor volume from one shot to the next.

## 3. Results

Variation of secondary divertor volume produces changes in a wide variety of plasma parameters. This section will examine only three of the variations as functions of $Z_X^S$:

1. the effect on the up/down balance of peak heat flux to the divertors,
2. the effective fueling rate of the core plasma and
3. the highest density achieved just before the H–L back transition.

Finally, a point comparison was done between an unbalanced DN plasma and a SN shape for which the sum of the $X$-point heights in the DN (i.e., the total length of the divertor legs) was equal to the $X$-point height (divertor leg length) in the SN.

### 3.1. Heat flux balance

Reduction of $Z_X^S$ did not produce a significant change in up/down balance of peak divertor heat flux until $Z_X^S$ dropped below a threshold value. This indicates that the distribution of power in the SOL is unaffected by $X$-point height variation until the high recycling character of one of the divertors is lost at small $X$-point height. The normalized peak heat flux in the secondary divertor as a function of $Z_X^S$ is shown in Fig. 2 for the pre-gas ELMing H-mode phase of unpumped plasmas. There is non-negligible variation in the up/down magnetic balance of the plasmas in this dataset. To compare the data fairly, each point in Fig. 2 represents the value expected for the same up/down magnetic balance of the equilibrium. The results of Petrie et al. [6] were used to factor out the variation in peak heat flux due to changes in up/down magnetic balance. Although this correction removes the large effect of variation in up/down magnetic balance, the data from high $X$-point height shapes in [6] may tend to slightly underestimate the expected peak heat flux value in the secondary divertor (overestimate the normalized value in Fig. 2) for low $X$-point heights. A value of 1.0 in Fig. 2 indicates the peak heat flux in the secondary divertor is the expected value [6] for $Z_X^S = 16$ cm, a value less than (greater than) 1.0 means the secondary divertor is getting less than (greater than) the expected heat flux. For high $Z_X^S$ the heat flux is the expected value consistent with the studies in [6]. As $Z_X^S$ was reduced, the normalized peak heat flux in the secondary divertor decreased. However, for low $Z_X^S$ the peak heat flux was significantly larger than the expected value.

These variations can be understood by considering the mapping of a flux tube which is one radial scale length of the power outboard of the primary separatrix at the midplane. As $Z_X^S$ is reduced the mapping of this flux tube to the secondary divertor shows greater flux expansion at the target plate and the peak heat flux decreases due to broadening of the profile on the target. This is the expected behavior [7] as long as the high recycling character of the divertor plasma is maintained as $Z_X^S$ is reduced. However, when $Z_X^S$ is reduced enough that this flux tube maps to the secondary divertor target with negligible divertor leg length, then the high recycling character of the secondary divertor is lost. With reduced recycling local temperatures (densities) would be expected to increase (decrease) and local volumetric radiation would be expected to decrease leading to higher peak heat flux on target. For the plasmas in this study, the midplane SOL scale length of the parallel heat flux is about 0.6 cm. At $Z_X^S = 2$–$3$ cm the leg length of this flux tube in the secondary divertor becomes negligible and the high recycling divertor is lost.

### 3.2. Effective fueling

The effective rate of rise of the core line-averaged density at the L–H transition increases as the volume of the secondary divertor decreases. This indicates that the fueling rate of the core plasma is increased for lower secondary $X$-point height. Data from shots with and without divertor cryo-pumping are shown in Fig. 3. The effective fueling source, $S_{\text{eff}}$, was obtained from an exponential fit to the increase in the total core particle content during the ELM-free period (approximately 400 ms) after the L–H transition. The contribution to the core fueling by the neutral beams, $S_{\text{nb}}$, was subtracted out to obtain the fueling contribution from around the separatrix. Finally, the values were normalized by midplane neutral pressure and core pedestal density to eliminate shot-to-shot variation in neutral and electron densities in the fueling region near the edge of the core plasma. Fig. 3 shows a clear trend to higher core fueling as $Z_X^S$ was reduced.

The trend in Fig. 3 suggests that ionization of neutrals from the secondary divertor region plays a significant role in fueling the core plasma for unbalanced DN configurations. In contrast to SN equilibria which have the secondary $X$-point well outside the vacuum chamber and particle recycling only in the primary divertor region, nearly up/down balanced DN configurations produce appreciable recycling flux in the secondary divertor. The plasmas in this study had the up/down magnetic balance shifted slightly toward the primary divertor and therefore the majority of the power flux went to the primary divertor. This means the secondary divertor plasma is colder than the primary, and recycled neutrals in the secondary have a high probability of

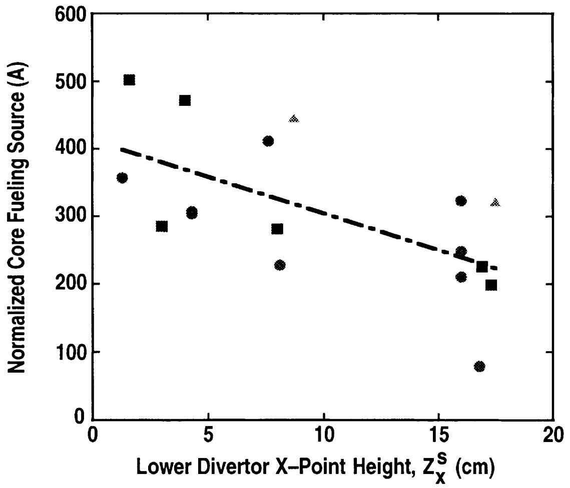


Fig. 3. Normalized core fueling source versus secondary $X$-point height for unpumped (circles), partially pumped (triangles) and well-pumped (squares) discharges. A substantial increase in fueling is seen as $Z_X^S$ decreases for all discharges taken together (dot-dashed) and for each dataset with constant pump conditions. Vertical scatter at fixed $Z_X^S$ and constant pump conditions shows evidence of changing wall conditions – effective fueling source increases with each successive repeat shot.

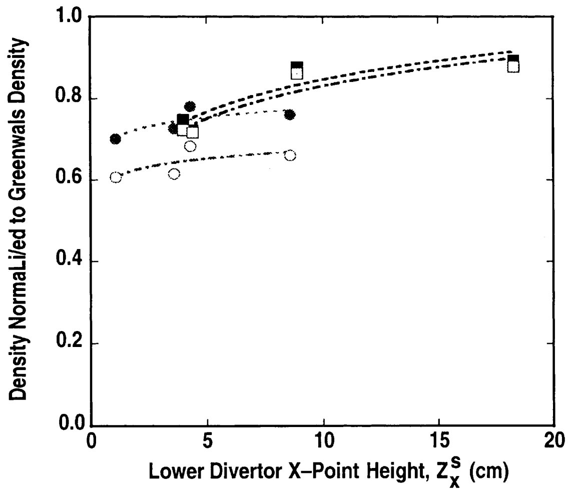


Fig. 4. Line-averaged (closed) and pedestal (open) densities at the H–L back transition normalized to Greenwald density versus $Z_X^S$ for unpumped discharges (circles) and pumped discharges (squares). All of these densities decrease as secondary divertor volume decreases. Pumping produced higher absolute density at the H–L transition than the unpumped cases.

reaching the edge of the core plasma. The trend in Fig. 3 is consistent with this picture and the expectation that the penetration probability of a neutral from the secondary divertor target into the core would increase with decreasing $Z_X^S$. However, $D_\alpha$ measurements show somewhat higher recycling in the primary divertor than in the secondary, consistent with the slightly upward magnetic balance and ion $\nabla B$ drift, and this ratio increases as $Z_X^S$ is reduced so neutrals from the primary divertor may also contribute to the trend in Fig. 3.

### 3.3. Density at H–L back transition

The maximum density that was obtained during ELMing H-mode in these discharges, before a back transition to L-mode, decreased as $Z_X^S$ was reduced. The line-averaged and pedestal densities [8] at the transition time are plotted as functions of $Z_X^S$ in Fig. 4 for both unpumped and pumped discharges. Both of these quantities decreased as $Z_X^S$ was reduced. The absolute density in the unpumped discharges was lower than with pumping at high $Z_X^S$. However, the density limit dropped more rapidly with $Z_X^S$ reduction in the pumped cases yielding similar results at low $Z_X^S$. The width of the edge density pedestal was larger in the unpumped plasmas indicating a greater penetration of neutrals without pumping.

The dominant physics that explains the trend in Fig. 4 is again the increase in neutral escape probability from the secondary divertor as $Z_X^S$ was reduced. In this case the effect of increased neutral ionization in the edge of the core is to lower the pedestal temperature for fixed core density as $Z_X^S$ was reduced thereby inducing the H–L back transition at lower core density. This also explains the higher density limit with pumping at moderate to high $Z_X^S$.

### 3.4. Comparison of optimized DN versus SN

A direct comparison of several ‘optimized’ unbalanced DN discharges with a comparable SN discharge shows that the DN shape has advantages for future tokamak operation. Performance parameters from three unbalanced DN discharges and a SN discharge, all at the same injected power, are shown in Table 1. The $X$-point height of the SN discharge was 16 cm. The DN shapes were optimized, in the sense of maximizing core volume while minimizing secondary peak heat flux (Fig. 2), by sharing the total $X$-point height between the primary and secondary divertors as $Z_X^P = 9$ cm and $Z_X^S = 7$ cm, respectively. The table shows that the advantages of the DN configuration over the SN shape are:

1. lower core fueling rate which should allow greater density control;
2. higher normalized performance, $\beta_N H_{89P}$ [9], in the ELM-free phase which might be exploited in advanced tokamak scenarios;
3. reduced outer leg peak heat flux which should make divertor design easier;
4. higher fraction of the Greenwald density achievable in H-mode for maximizing fusion power.

Table 1
Comparison of performance parameters from SN and optimized DN discharges with comparable total divertor $X$-point height

| Parameter | SN reference shot 98397 | Optimized DN shot 98392 | Optimized DN shot 98393 | Optimized DN shot 98394 |
|---|---|---|---|---|
| $S_{eff}$ at L–H transition (normalized) (A) | 289 | 25–80 | 40 | 126 |
| Maximum $\beta_N H_{89P}$ | 3.77 | 9.14 | 7.16 | 4.83 |
| Maximum outer leg heat flux ($MW/m^2$) | 3.32 | 1.78 | N/A | 1.25 |
| Line-averaged $n_e$ at H–L back transition/ Greenwald density | 0.72 | N/A | 0.74 | 0.90 |
| Wall conditions | Saturated; acts as source | Depleted, pumping | Neutral, gas injection later | Saturated, acts as source |

This comparison also pointed out the importance of wall conditions in these discharges. The performance of the three DN discharges was somewhat different even though they were as nearly identical as possible in terms of shape, injected power, and current. The first DN plasma came after a set of discharges with no supplemental gas injection so the walls were probably depleted and pumping. The next plasma in sequence had substantial gas injection in the latter phase to bring the density to the H–L back transition. This probably saturated the walls so that in the final discharge the walls were acting as a source. The effective fueling rates and maximum $\beta_N H$ in these three shots clearly show the effect of the wall source.

## 4. Discussion and future work

Results obtained in this study and those in [5,6] show that for high-$\delta$ operation an unbalanced DN plasma shape has some advantages over a SN shape for future high power tokamak operation. However, maximizing the core plasma volume by minimizing the secondary divertor volume, in an attempt to achieve the performance advantages of a high-$\delta$ unbalanced DN configuration, produces both positive and negative effects on performance. The advantage of having the secondary divertor share some of the SOL heat flux was not strongly degraded by reduction in the secondary divertor volume provided the secondary $X$-point was well inside the vessel. As $Z_X^S$ was reduced the peak heat flux in the secondary divertor actually decreased somewhat due to flux expansion. Secondary peak heat flux increased only when the flux surface that was one SOL power scale width from the primary separatrix at the midplane was seen to have negligible divertor leg length in the secondary divertor and the high recycling character of the divertor was lost.

The advantages for core performance of greater volume, elongation and safety factor at constant current as $Z_X^S$ is reduced are partially offset by degradation of other core performance measures. The effective rate of rise of the core $n_e$ at the L–H transition increased and the line-averaged $n_e$ at the H–L back transition decreased as secondary $X$-point height decreased. This was due to reduced screening of neutrals from the core as $Z_X^S$ decreased. These trends in combination effectively reduce the core plasma density operating window monotonically with $Z_X^S$ reduction. For steady state scenarios the reduction in fueling control may outweigh advantages of greater volume and current capability. For high neutron flux scenarios the change in fusion rate scales linearly with volume and as the square of the density so that even though the reduction in density limit is small this may more than offset the advantage of larger volume.

The direct comparison of a SN discharge with several comparable optimized unbalanced DN discharges showed that a carefully selected DN shape may still perform better than a SN shape with the same divertor height. However, more work must be done in this area to achieve an unambiguous comparison because uncontrolled factors such as wall conditions were playing a role in the comparison discharges in this study.

## Acknowledgements

Work supported by US Department of Energy under Contract Nos. DE-AC03-99ER54463, W-7405-ENG-48, DE-AC05-00OR22725, and DE-AC04-94AL85000.

## References

[1] ITER Physics Basis Editors et al., Nucl. Fus. 39 (1999) 2137.
[2] T.H. Osborne et al., Plasma Phys. Control. Fus. 42 (2000) 1.
[3] E. Lazarus et al., in: Proceedings of the 15th International Conference on Plasma Physics and Controlled Nuclear Fusion Research, Seville, Spain, 1994, vol. 1, International Atomic Energy Agency, Vienna, 1995, p. 609.
[4] H. Zohm et al., Plasma Phys. Control. Fus. 38 (1996) 1497.
[5] T.H. Osborne et al., these Proceedings.
[6] T.W. Petrie et al., these Proceedings.
[7] A. Loarte, P.J. Harbour, Nucl. Fus. 32 (1992) 681.
[8] R.J. Groebner, T.H. Osborne, Phys. Plasmas 5 (1998) 1800.
[9] P.N. Yushmanov et al., Nucl. Fus. 30 (1990) 1999.